Journal of Building Engineering 45 (2022) 103445

Contents lists available at ScienceDirect

Journal of Building Engineering

journal homepage: www.elsevier.com/locate/jobe

Joint strengthening by external bars on RC beam-column joints

Joaquín G. Ruiz-Pinilla [a,*], Antoni Cladera [a], Francisco J. Pallarés [b], Pedro A. Calderón [b], Jose M. Adam [b]

[a] Department of Industrial Engineering and Construction, University of the Balearic Islands, Palma, 07122, Spain
[b] ICITECH, Universitat Politècnica de València, Valencia, 46022, Spain

ARTICLE INFO

Keywords:
Seismic upgrading
Beam-column joint strengthening
Steel caging
Gravity loads
Cyclic loads

ABSTRACT

Column strengthening is a very common practice for improving the seismic performance of reinforced concrete frame structures or repairing damage after a seismic event. Several methods are employed for column strengthening, which can improve column strength by preventing its shear, bending or compression failure. However, not all methods allow column strengthening connections between adjacent floors, thus the beam-column joint strength could be limited by the column-joint interface capacity. This work aimed to analyse two joint strengthening designs, for which an experimental campaign of eight full-scale beam-column joints strengthened with steel caging, and subjected to cyclic and gravity loads, was carried out. As access to joint panels is very complex in existing structures, joint strengthening consists of external solutions: vertical or diagonal bars and capitals connecting columns. The results showed that these techniques significantly increased beam-column joint strength and highlighted that failure can be undesirably transferred to the joint. Vertical bars prevented the bending failure of the column-joint interface, but failure occurred at the joint in this study. Diagonal bars can also prevent joint failure.

1. Introduction

Ageing infrastructures and the vulnerability of structural elements not explicitly designed to deal with seismic loads render it convenient to strengthen the most critical elements of many existing structures, which means that the safety and service life of constructions can increase. Seismic events are still causing serious human and material losses [1]. According to [2], for the period between 1980 and 2009, around 61.5 million people were affected by earthquakes and almost 400,000 of them lost their lives. Some most recent earthquakes have caused significant damage to reinforced concrete (RC) constructions, namely, among others: Sivrice, Turkey in 2020 [3]; Lorca, Spain in 2011 [4]; Van, Turkey in 2011 [5,6]; L'Aquila, Italy in 2009 [7]; Kashmir, Pakistan in 2005 [8]; Molise, Italy in 2002 [9].

In order to study construction deficiency implications in the seismic response, some authors [10–12] have performed shake table tests on small-scale RC frame structures. However, not only earthquakes can place constructions at risk; the passing of time exposes materials to a tough durability test; carbonation and chloride attacks impair RC structures' performance [13,14]. Concrete cracking and spalling and the reduction of bond and cross-section of reinforcement can result in brittle failures and unexpected structural collapses [15,16].

The most widespread techniques used for strengthening RC columns are steel caging [17–20], fibre-reinforced polymers [21,22], and concrete jacketing [23]. Some recent studies have employed hybrid elements [24] and shape memory alloys [25,26]. However, when it is necessary to improve a structure's response to horizontal actions, applying strengthening to columns is not enough, and we need to pay attention to the beam-column joint (henceforth referred to as BCJ), which is subject to major efforts in a very small area [27]. Joint behaviour has considerable implications for the structural response [28,29], especially when the structure is designed to resist only vertical loads [30] and the joints do not have transverse reinforcement [31]. BCJ have been identified as potentially one of the weakest components of RC frame structures subjected to seismic loads. A severe damage within the joint may trigger deterioration of the overall performance of the BCJ. Kim, J. et al. (2012) [32] have constructed an extensive experimental database classified by governing failure mode sequence, and proposed the key points in stress-strain curves for prediction models. Indeed several works have been carried out to apply strengthening to BCJs [33] with different materials: composite materials [34–40], steel [41–50] or concrete [51–53].

* Corresponding author.
E-mail address: joaquin.ruiz@uib.es (J.G. Ruiz-Pinilla).

https://doi.org/10.1016/j.jobe.2021.103445
Received 14 June 2021; Received in revised form 4 October 2021; Accepted 8 October 2021
Available online 14 October 2021

The authors of the present work undertook a previous experimental campaign [54] consisted in seven full-scale RC BCJs not originally designed to resist horizontal loads, where columns were strengthened externally by steel caging. Two methods to connect the column jacket to the joint by steel capitals were analysed. The obtained results revealed that the strengthening technique improved the BCJ's strength to horizontal loads. Therefore, as no connection was employed between the top and bottom columns through the joint, the maximum load was limited by the column's bending moment capacity at its interface with the joint, when no axial load was applied to columns.

The paper presents the results of a new experimental campaign that included two new BCJ strengthening types that connected the top and bottom columns. These techniques were based on vertical and diagonal steel bars to connect column strengthening across the joint. Hence columns gained continuity and column bending capacity increased, but more attention should be paid because BCJ failure was relocated from, in some cases, the column-joint interface to the joint core. The joint strengthening design poses a considerable challenge: finding a way to increase the bending moment of the column-joint interface by connecting the column jacket through the joint without either replacing the failure in the joint without damaging the joint drilling holes in it, which is also economic, easy and quick to apply and barely increases the space needed to invade around the column.

2. Experimental program

The complete experimental program included eight full-scale interior RC BCJs designed for gravity loads only, as in the typical buildings constructed in Spain in the 1980s–1990s. None of the specimens complies with the design principles of current earthquake codes because non-ductile details were considered. The geometry and steel reinforcement configuration of both the column and beam were the same as those considered in a previous work [54]. Thus the control specimen (*A.W.L0*) was common to both these experimental campaigns.

2.1. Specimens design

All the specimens were internally reinforced in the same way (Fig. 1), and the steel cage that was placed externally on columns was also the same in them all (Fig. 2). The difference between the tested specimens lay only in the way joints were strengthened. A former Spanish code EH-80 [55] has been used for designing the specimens. Specimens' characteristics are seen in Table 1. Specimen *A.W.L0* was the control BCJ, in which the joint was not strengthened. *VB* and *DB* were the vertical and diagonal exterior bars, respectively. These rebars were screwed to capitals. *L0* and *L1* indicate the axial load level applied to the column: *L0*, without axial load ($\nu = 0$), and *L1* with a normalised axial load equalling $\nu = 0.3$. Some specimens were constructed and tested in duplicate (tests -1 and -2) to ensure the reliability of the results, which involved eight tests with five different configurations. The discussion in Section 3.3 includes two additional specimens from [54] to gain a better understanding of the exterior strengthening effect. These additional specimens were called *A.C.L0* and *A.C.L1,* and had steel capitals like the specimens strengthened with the exterior bars from Table 1, but with no connections between them (no vertical or diagonal bars).

Specimens were made of 2200 mm-long columns with a 300 × 300 mm cross-section, and 3300 mm long-beams with a 300 × 400 mm cross-section (Fig. 1). The steel boxes made with UPN profiles and welded plates, Ø16 mm corrugated bars and hinge devices, were placed on the end of the beam and columns to connect the specimen to the test frame. The distance between inflexion points was 4000 mm in beams and 2800 mm in columns.

Test specimens were manufactured with medium-low performance concrete. The mean strength obtained from testing cylindrical compressive specimens was between 23.2 and 28.5 MPa. Tests were run on the same day as the test performed with the corresponding specimen. Two cylindrical specimens were tested for each beam-column joint specimen.

B500SD steel was used: yield and ultimate strength of 550/660 MPa for Ø12 mm reinforcement and 570/675 MPa for Ø16 mm, respectively. Columns were longitudinally reinforced by using four Ø12 mm deformed steel rebars. Transverse reinforcement consisted of 6 mm diameter steel stirrups, 150 mm spaced. The upper and lower beam reinforcement quantities were asymmetric. The upper longitudinal reinforcement was 2Ø12 and the lower one was 2Ø16 (both types overlapping at the joint core at 250 mm). Three more continuous Ø16 steel upper rebars were placed to continuously cross the joint. Transverse beam reinforcement was Ø8 mm, 100 mm spaced. No stirrups were

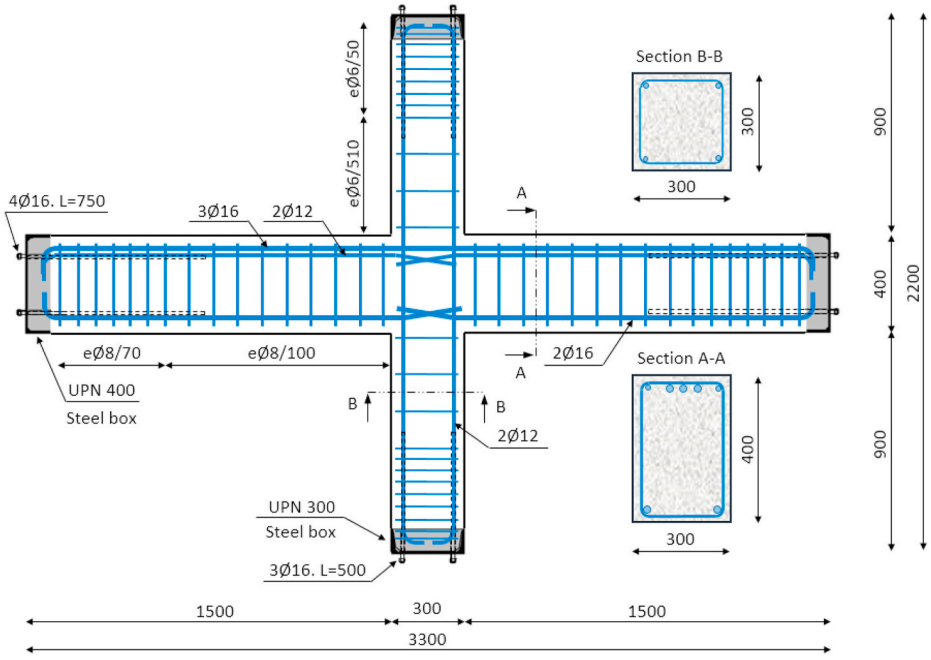

Fig. 1. Specimen geometry and reinforcement (dimensions in mm).

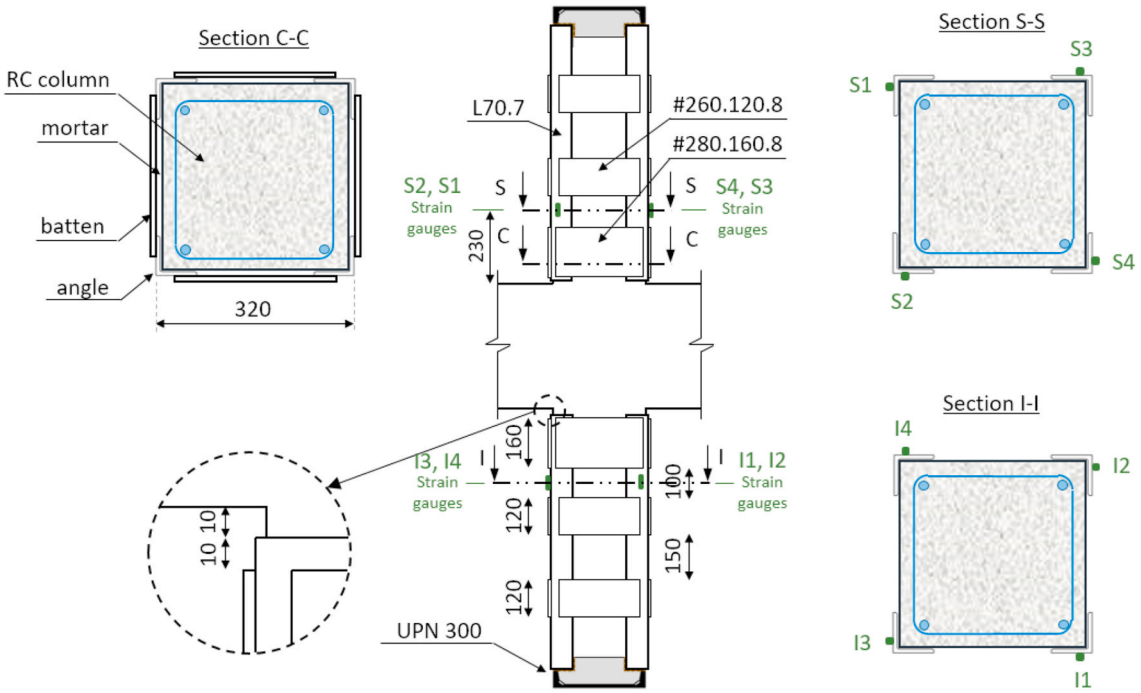

Fig. 2. Steel caging disposition and strain-gauges for the axial strain measurements in angles (dimensions in mm).

Table 1
Number and characteristics of the tested specimens.

N°	Specimen	f_c [MPa]	Joint strengthening	Axial load ($N = \nu \cdot A_c \cdot f_c$) [kN]
1	*A.W.L0*	23.2	–	0
2	*A.VB.L0-1*	27.4	Capital + Vertical Bar	0
3	*A.VB.L0-2*	24.5	Capital + Vertical Bar	0
4	*A.VB.L1*	27.5	Capital + Vertical Bar	740
5	*A.DB.L0-1*	22.4	Capital + Diagonal Bar	0
6	*A.DB.L0-2*	22.2	Capital + Diagonal Bar	0
7	*A.DB.L1-1*	28.5	Capital + Diagonal Bar	765
8	*A.DB.L1-2*	28.3	Capital + Diagonal Bar	765

arranged on the joint, and the concrete cover of beams and columns was 25 mm.

2.2. Strengthening techniques

The columns of all specimens were strengthened by the same configuration. Four steel angles and battens were placed around the RC columns, as Fig. 2 shows. Angles were welded to the steel box at the end of the column on one side, and angles were free on the other side. All the steel elements were S275 (yielding strength = 275 MPa). The contact between the steel cage and concrete was guaranteed by cement mortar (1/2 cement/sand ratio). This configuration was designed after analysing the previous research performed at the ICITECH (Universitat Politècnica de València) [18,20,56,57]. Angles were L70.7 mm, and battens were 260x120 × 8 mm and 280x160 × 8 mm for the nearest one to the joint.

A reference specimen (*A.W.L0*) was not strengthened at the joint, while others were strengthened in two different modes: with vertical bars or diagonal bars (Fig. 3). The steel used for these bars was B500SD Ø16 mm (yielding and ultimate strength of 560/660 MPa, respectively), in which threads were cut at each bar end to fix capitals with nuts. Each capital was welded to the steel cage on three borders: one longitudinal along the capital and batten, and two transversal ones between the capital and steel angles.

2.3. Test setup

Specimens were fixed to the test frame by four hinges on each end of columns and beams, and were subjected to a quasi-static cyclic loading test that included gravity and horizontal loads (Fig. 4 and Fig. 5). Gravity loads were applied to the column by a 1000 kN hydraulic actuator at the top (representing the top and ground floors of a building;

a. *W typology. No connection.* b. *VB typology. Vertical bar.* c. *DB typology. Diagonal bar.*

Fig. 3. Joint strengthening.

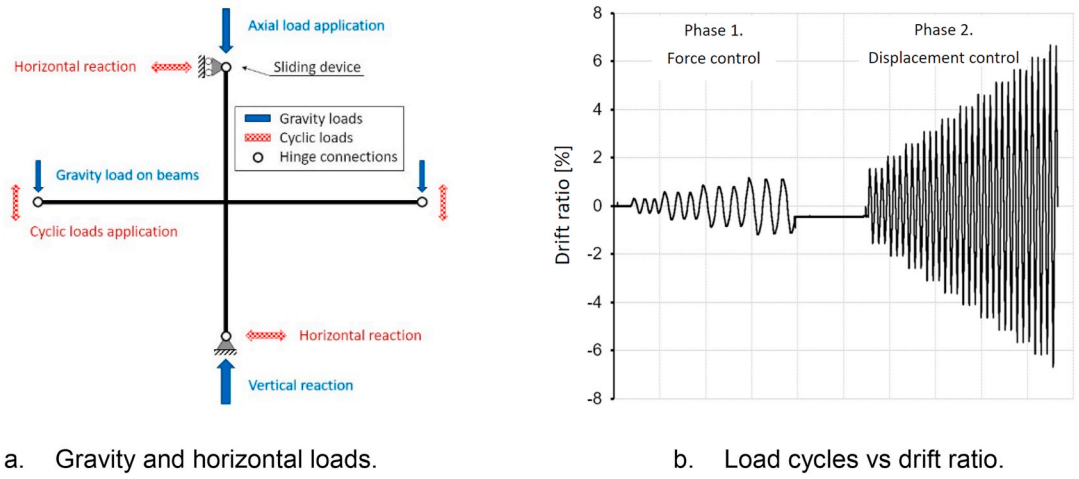

Fig. 4. Loads applied to specimens.

Fig. 5. Specimens inside the test frame ready for testing.

axial load is found in detail in Table 1), and on beams by two double effect hydraulic actuators (set at 30 kN to simulate slab loads). Authors like [37,58,59] have also considered gravity loads on beams. Reversed cyclic loads were applied with varying drift to the main beam up to specimen failure by keeping ends of columns fixed in the horizontal direction (Fig. 4b).

For the cyclic load, two phases were implemented by the beam-ends loading specimen (BL method [60]). First one was run by force control. After applying the gravity load to beams, the load on each beam was incremented (or decremented) in opposite directions, thus the total gravity load on the specimen remained constant. With a 1% drift ratio, when the non-linear effects started to have a stronger impact, the control of the horizontal loads was changed to the displacement control. The combination of both phases needs the correct coordination of movements [54]. Each cycle was repeated 3 times to accomplish specimens' stiffness degradation.

2.4. Test instrumentation and measurements

Internal beam and column reinforcement, external vertical steel angles and external strengthening bars were monitored by strain-gauges at different points.

The four rebars of the RC column were monitored (Fig. 6). On two bars (*C2 and C3*), five strain-gauges (Pos −2, Pos −1, Pos 0, Pos 1, Pos 2) were placed. On the two other bars (*C1* and *C4*), only two strain-gauges were placed (*Pos -1* and *Pos 1*). On beams, corner rebars *BA2* and *BA3* (non-continuous bars) were monitored at the beam-joint intersection (positions *Pos -1* and *Pos 1*), while two of the corner rebars (*BA3* and *BA4*) and the continuous rebar (*BAC*) were monitored at seven positions. The four steel angles of each column were monitored with the strain-gauges on two sections between two battens at a distance of 230 mm from the column-joint interface (section S-S and section I-I, Fig. 2). Each external bar was also monitored with one strain-gauge at the midpoint.

3. Experimental results and discussion

3.1. Hysteretic response and failure modes

Fig. 7 shows the hysteretic curves and failure modes obtained during the tests for the five different configurations. The hysteretic shear load on the column *versus* the relative displacement is represented on the left. The state of the specimens at the 3.5% drift ratio for the test without gravity load on the column and the 2.5% drift ratio for the specimens with the axial load is shown on the right. These percentages have been

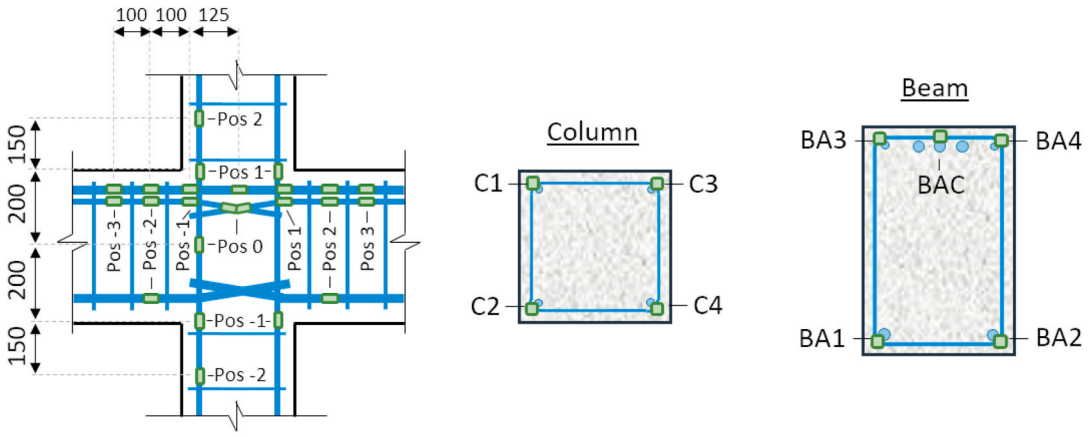

Fig. 6. Monitoring internal reinforcement.

set to be able to compare the crack patterns between different specimens. Specimens with axial load show lower value since they have brittle behaviour and damage occurs earlier. When two identical tests were carried out, only one specimen was shown (see Fig. 7) given the similar obtained results.

From Fig. 7, we can see major differences between the tested specimens. A strong pinching effect was noted on the specimens without axial load on columns (specimens *L0*) (Fig. 7a, b, Fig. 7c), but they showed excellent ductility. The specimens with the axial load (specimens *L1*) evidenced greater strength, but less ductility (Fig. 7d and e).

Crack patterns significantly differed in each test. With specimen *A.W.L0* (Figs. 7a and 8a), cracks concentrated at the column-joint interface due to the column reinforcement yielding in this zone.

The external vertical bars and capitals (Figs. 7b and 8b) incremented the bending capacity in this zone, where the steel caging ended and allowed strengthening continuity through the joint between the top and bottom columns. Therefore, no large cracks were observed at the column-joint interface. Instead failure was transferred inside the joint, which was seriously damaged. On the *A.VB.L0* specimens (only specimen *A.VB.L0-1* is shown in these figures), diagonal cracks developed at the joint and joint's shear deformation are seen in Figs. 7b and 8b.

When external diagonal bars were installed instead of vertical bars, once again the crack pattern changed completely: cracks developed at the beam-joint interface due to these sections' bending capacity, and no significant damage was observed on the joint (Figs. 7c and 8c).

When an axial load was applied to the column, failure took place at the joint by shear and compression cracks (Fig. 7d, e, Fig. 8d and e), regardless of whether the external reinforcing bar was installed diagonally or vertically. When *A.DB.L1-2* testing finished, the disaggregated concrete of the joint core was removed to check the size of the affected area and reinforcement bucking. As Fig. 8f depicts, the affected area was bigger than the original joint, which indicates that capitals allowed joint size to increase, which improved its strength capacity.

The general results obtained while testing are summarised in Table 2: the maximum shear load applied to columns in both loading directions (V_c^+, V_c^-), the relative displacement for the max load in each direction (Drift$^+$, Drift$^-$), the mean shear value ($V_{cm} = ½\cdot(V_c^+ + V_c^-)$) reached in both directions and the drift ratio for 15% loss of maximum strength ($Drift_{85\%}$). The V_c^+ values were a few kN larger than the V_c^- values, because of the relative position of the overlapped rebars inside the joint. In one loading direction, the overlapped reinforcement had more concrete cover than in the other direction, as explained in [54] and shown in Fig. 8f.

The envelopes of hysteretic curves are shown in Fig. 9. V_1 and V_2 are the loads on the beams end by the left-hand and right-hand actuator, respectively. As the gravity load on beams was 30 kN, the V_1 and V_2 values started from the drift ratio 0% value at the beginning of the test. Fig. 9 shows that all the tested specimens achieved marked strength increments in relation to the reference specimen. When no axial load was applied to columns, the use of exterior vertical or diagonal bars increased strength by around 2.5-fold (2.58 for *A.VB.L0-1* and 2.48-fold for *A.VB.L0-2*) and 2.2-fold (2.15 for *A.DB.L0-1* and 2.29-fold for *A.DB.L0-2*), respectively. Vertical or diagonal bars configurations achieved similar strengths when the axial load was applied to the column. The incremented BCJ strength when the axial load was applied was about 1.3-fold in the specimens with vertical bars and 1.4-fold in the specimens with diagonal bars, compared to the situation in which no axial load was applied to strengthen specimens. Note that the results in Table 2 and Fig. 9 for the companion specimens (*A.VB.L0-1* and *A.VB.L0-2*; *A.DB.L0-1* and *A.DB.L0-2*; *A.DB.L1-1* and *A.DB.L1-2*) are similar for each test configuration, which confirms the repeatability of our test results.

3.2. Energy dissipation and stiffness

The results obtained from the cumulative energy dissipated during the test are shown in Fig. 10a. The reference specimen is that which dissipated the least energy. This diagram reveals that BCJ strengthening significantly increased the total dissipated energy when no axial load was applied. When axial load was applied, not so much energy was dissipated because specimens failed earlier.

The mean value of the stiffness for the *i*th cycle is shown in Fig. 10b. The reference specimen exhibited more abrupt stiffness decay after the 1% drift ratio and the specimen lost more than 50% of its initial stiffness. Stiffness degradation was slighter for the other specimens. BCJ strengthening increased specimens' stiffness considerably, more than 1-fold after the 1.5% drift ratio, but no significant differences were found between external vertical or diagonal bars. When axial load was applied to columns, stiffness increased slightly, but degradation occurred more quickly than in the other tests.

3.3. Reinforcement behaviour

Fig. 11 compares the strain at the top continuous reinforcement of the beam (*BAC rebar*) and column (*C rebar*) for each joint strengthening type at the 1% drift ratio. One axis represents the distance in metres from the measurement points to the beam-column axis, while the other axis represents the reinforcement strain (negative value means tension). Fig. 11 includes the results of specimens *A.W.L0, A.C.L0* and *A.C.L1* of [54] to better compare the effect of exterior strengthening on reinforcement behaviour. Unfortunately, we were unable to record the data of some measurements due to the severe damage of the concrete area where gauges were placed.

The beam reinforcement behaviour observed during this

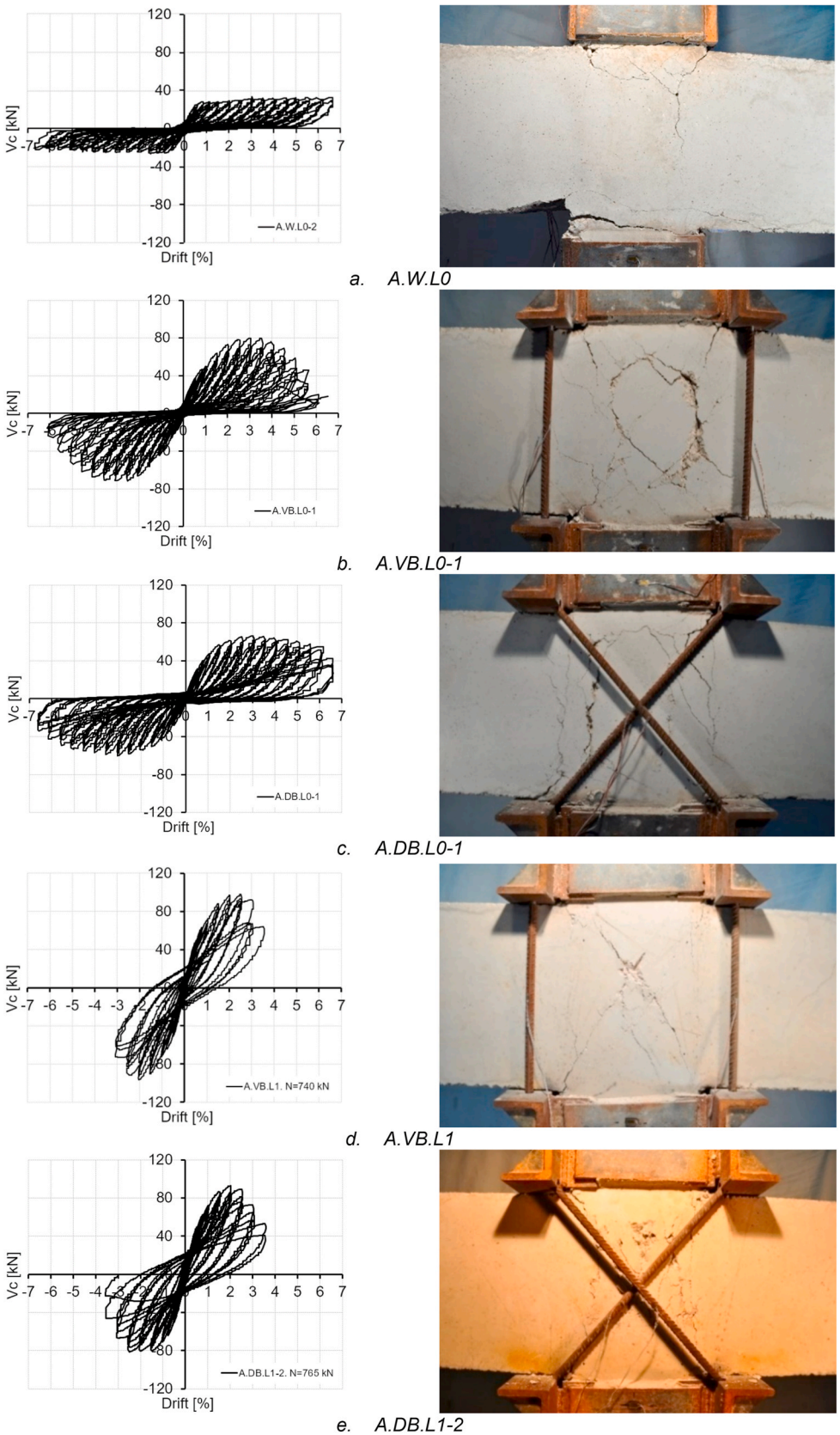

Fig. 7. Left: column shear force vs. drift ratio. Right: joint view at the 3.5% drift ratio in the specimens without axial loads on columns (L0), and the 2.5% drift ratio in those with the axial load (L1).

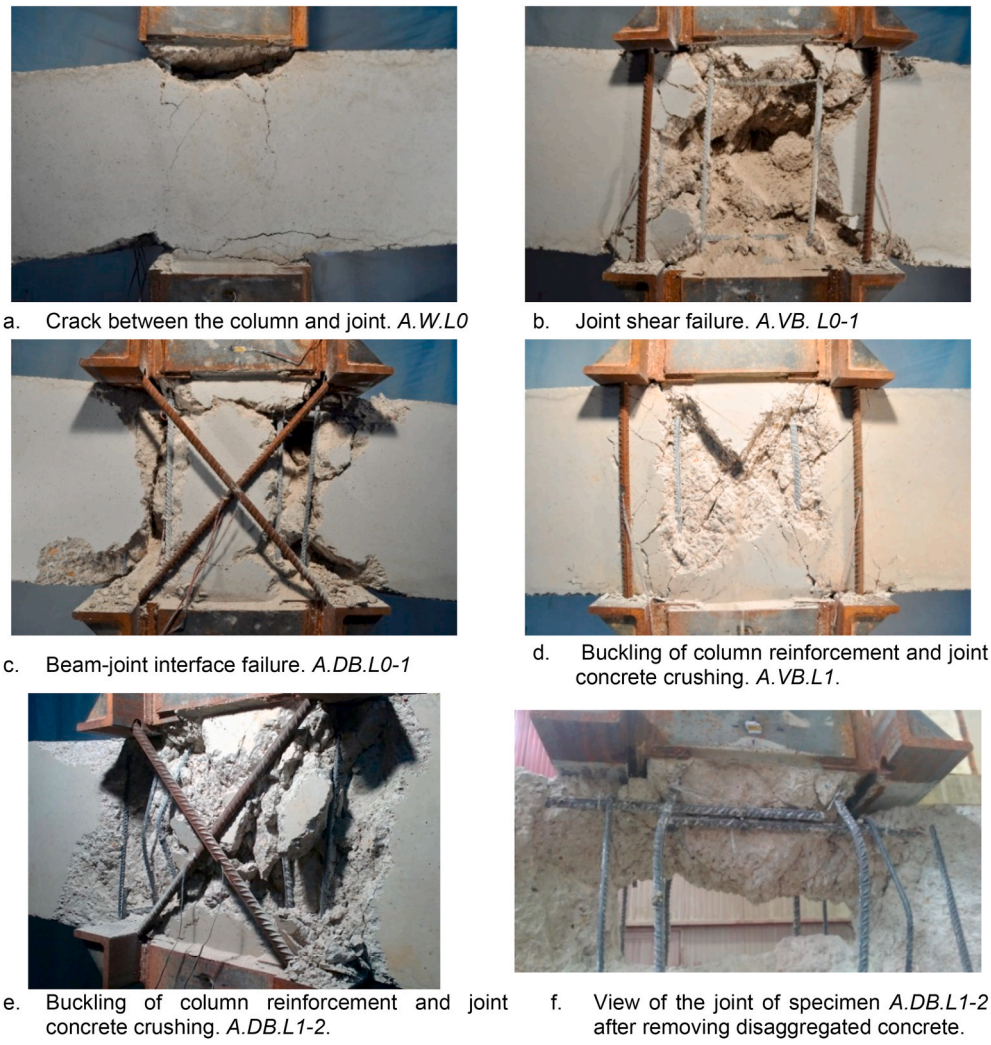

Fig. 8. Joint damage after the last load cycle.

Table 2
General test results.

Specimen	V_c^+ [kN]	V_c^- [kN]	Drift$^+$ [%]	Drift$^-$ [%]	V_{cm} [kN]	$Drift_{85\%}$ [%]
A.W.L0	32.7	−25.9	5.5	−1.5	29.3	>6.5
A.VB.L0-1	79.5	−71.8	3.5	−2.5	75.7	4.56
A.VB.L0-2	78.4	−66.8	2.5	−3.0	72.6	4.74
A.VB.L1	97.8	−95.9	2.5	−2.0	96.9	2.74
A.DB.L0-1	66.4	−59.7	3.0	−3.0	63.1	5.47
A.DB.L0-2	68.4	−65.8	2.5	−3.0	67.1	4.94
A.DB.L1-1	98.6	−91.5	2.5	−2.0	95.1	2.92
A.DB.L1-2	92.7	−81.1	2.0	−2.5	86.9	2.85

experimental campaign was similar to the results obtained in [54]: (1) after the first cycles, the continuous top reinforcement (*BAC*) strain was the same through the joint when gravity load was applied; (2) discontinuous reinforcement (*BA4* and *BA1*) no longer overlapped due to loss of adherence; (3) axial load applied to the column favoured the adherence of beam reinforcements.

When the top reinforcement was submitted to tension on the right side of the joint, tension remained almost constant through the joint because adherence degraded and reinforcement worked almost like a tie when no axial load was applied (Fig. 11a). Instead, when axial load was applied to the column, the reinforcement adherence in the joint was much better preserved (Fig. 11b).

The use of exterior bars modified the anchoring of beam reinforcements. As seen in (Fig. 11a), the strain on the *BAC* reinforcement on the left side of the joint was lower in those specimens in which exterior bars were employed. It is worth noting that the load to which the specimens with external bars were subjected was higher than it was for others. This fact implies that for the specimens without axial load, adherence was better preserved when vertical or diagonal exterior bars were employed.

Fig. 11c shows the importance of external strengthening bars on column reinforcement behaviour. When no exterior bars were used (*A.C.L0*), the max strain of internal reinforcement went deep into the joint. This means that adherence had degraded. Note that the load applied to elements with external strengthening bars was higher than for the specimen. Consequently, exterior strengthening bars significantly reduced the column internal reinforcement strain. However, no significant differences were observed in column internal reinforcement behaviour when axial load was applied to the column (Fig. 11d). The column reinforcement strain represented in Fig. 11c and d was calculated as the average strain at rebars C2 and C3.

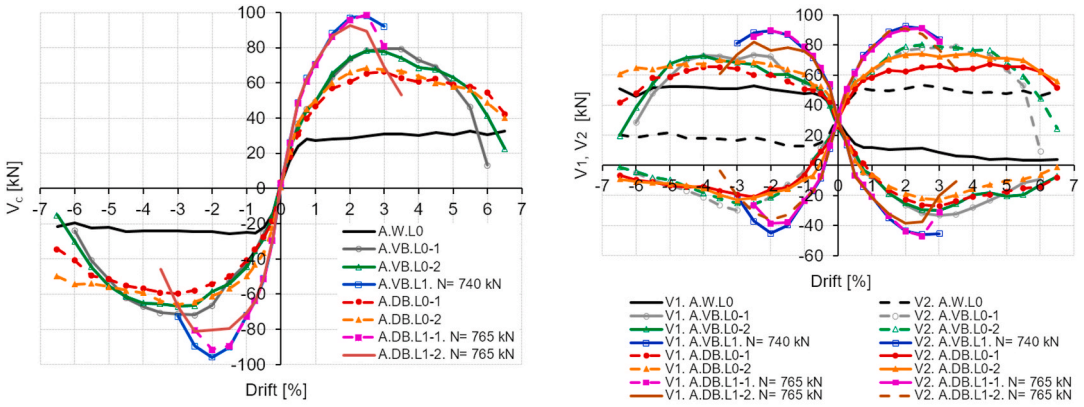

a. Shear force on columns vs. drift. b. Shear force on beams vs. drift.

Fig. 9. Envelope forces vs. drift.

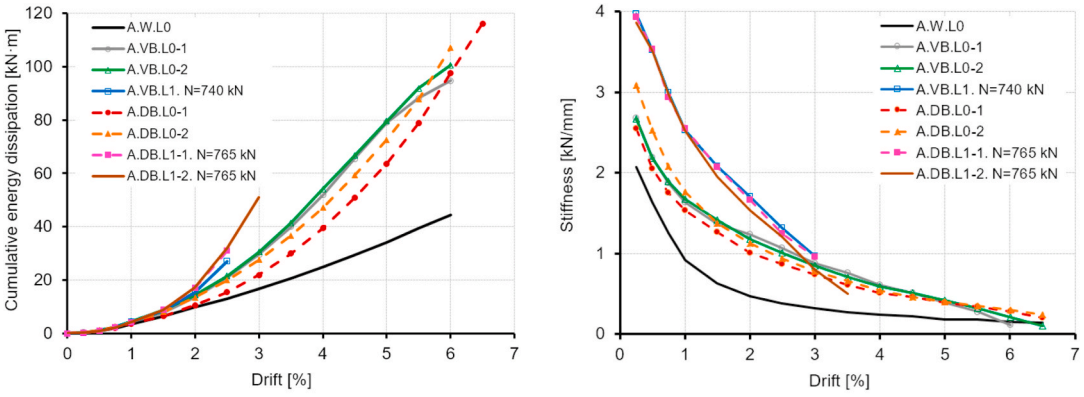

a. Energy dissipation vs. drift b. Stiffness vs. drift

Fig. 10. Cumulative energy dissipation and stiffness degradation after the three cycles of each drift.

3.4. Steel cage behaviour

Fig. 12 compares the strain at the steel angles of all the tested specimens. To better compare curves, and thanks to the symmetry of the specimens and loads applied to them, each curve was obtained by the mean value of the eight strain-gauges placed on steel angles (Fig. 2). This single curve per specimen was accomplished by computing the average of two curves (not plotted in Fig. 12). The first curve represents the average of the readings of strain gauges S1, S2, I1, I2 (steel angles compressed with a positive drift). The second curve represents the average of the readings of strain gauges S3, S4, I3, I4 (steel angles compressed with a negative drift). Bearing in mind that both curves represented the same phenomenon, but in opposite directions (symmetry vs. Y-axis), the sign of the second curve's drift was inversed to compute the average of both curves. Thus one curve in Fig. 12 represents the average behaviour of steel angles in tension and compression obtained by the eight strain gauges. A negative strain means tensile stresses.

High tension-compression symmetry was observed for the steel angles of those specimens without axial loads (*L0* - Fig. 12a). This figure depicts how the reference specimen (*A.W.L0*) angles presented a lower strain than in the other specimens because the steel cage was not colligated to the joint upon compression or tension if no external strengthening bars were added. In this case, tension or compression forces were transmitted to the steel cage only by the friction between angles and the column surface. With the specimens for which capitals were used (all the specimens, except *A.W.L0* - Fig. 12a), steel angles achieved a higher compression strain, which was even bigger when axial load was applied (*L1* - Fig. 12b). With the specimens for which external bars were used (either vertical or diagonal), steel angles achieved a higher tension strain.

The participation of the steel cage in specimens' response was estimated by the strain-gauge measurements. The bending moment participation of the angles at which strain-gauges were placed (Fig. 2) was obtained by multiplying the measured strain by the modulus of elasticity, by the angle cross-section and by the distance to the column axis.

Fig. 13 shows the contribution of steel angles and the RC column to axial-bending loads. On the left: bending moment value in the section where strain-gauges were placed (*M.Total*), bending moment supported by angles (*M.Angles*, estimated from strain values), bending moment supported by the RC section of the column (*M.RC*, calculated from the difference between *M.Total* and *M.Angles*). The right-hand column in Fig. 13 indicates: the percentage of the participation of angles and the RC section in relation to the total bending moment of the aforementioned section. The data from the twin specimens were averaged to display a single plot of the estimation per configuration in Fig. 13.

The bending capacity of the RC column (*M.MaxRC*) was obtained experimentally from the test done with the control specimen by multiplying the maximum horizontal force (Fig. 9a, Table 2) by the distance to the column/joint intersection where longitudinal reinforcement yielding occurred (Fig. 11). This bending capacity of the RC column is given in Fig. 13 by a dashed red line for the specimens without axial load

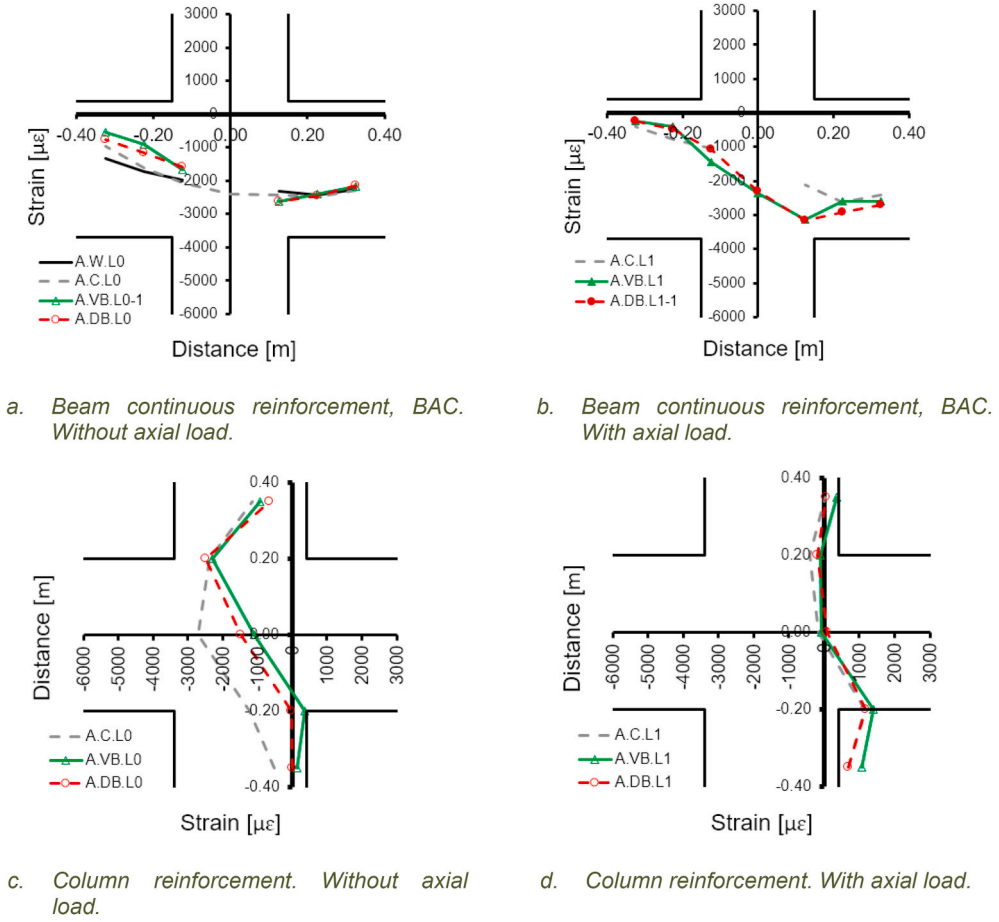

a. Beam continuous reinforcement, BAC. Without axial load.

b. Beam continuous reinforcement, BAC. With axial load.

c. Column reinforcement. Without axial load.

d. Column reinforcement. With axial load.

Fig. 11. Strain on the reinforcement of the beam and column at the 1% drift ratio.

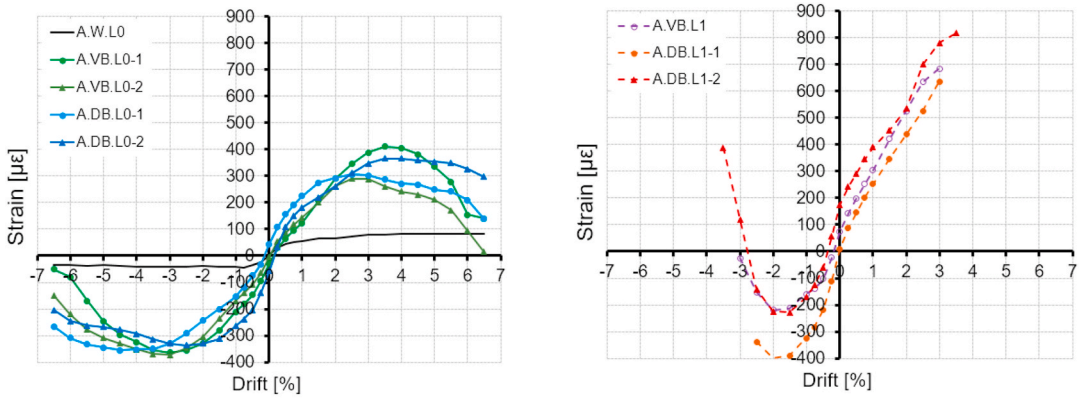

a. Specimens without axial load.

b. Specimens with axial load.

Fig. 12. Mean strain envelopes measured by the strain-gauges on steel angles (see Fig. 2).

(*L0*). In the section under study, it is worth noting the maximum bending moment capacity of the RC column estimated by the strain at the steel angles (*M.RC*) math with the real tested maximum bending moment (*M. Max RC*). This dashed red line is not plotted for the *L1* specimens because no direct experimental data are available about the RC column's axial-bending capacity (no non-strengthened specimen with axial-bending failure of the RC column was tested).

According to the results, the maximum bending moment that the RC column supported was 29 kN m (*M.Total* on Fig. 13a) and, thanks to the capitals and exterior bars, this value increased by around 2- or 3-fold.

Despite the control specimen not having either capitals or exterior bars, it should be noted that the contribution of steel angles to the column's bending capacity ranged between 21 and 28%. In the other specimens, the participation of angles started around 40% and rose to 60% with the drift ratio. These results indicate that both capitals and external bars were very important for the steel cage's effectiveness and its bending contribution increased as concrete was damaged.

Fig. 14a and Fig. 14b show the strain of the steel angles of the specimens strengthened with exterior bars under the axial load applied to columns. The Y-axis (ordinate) represents the strain of the angles at

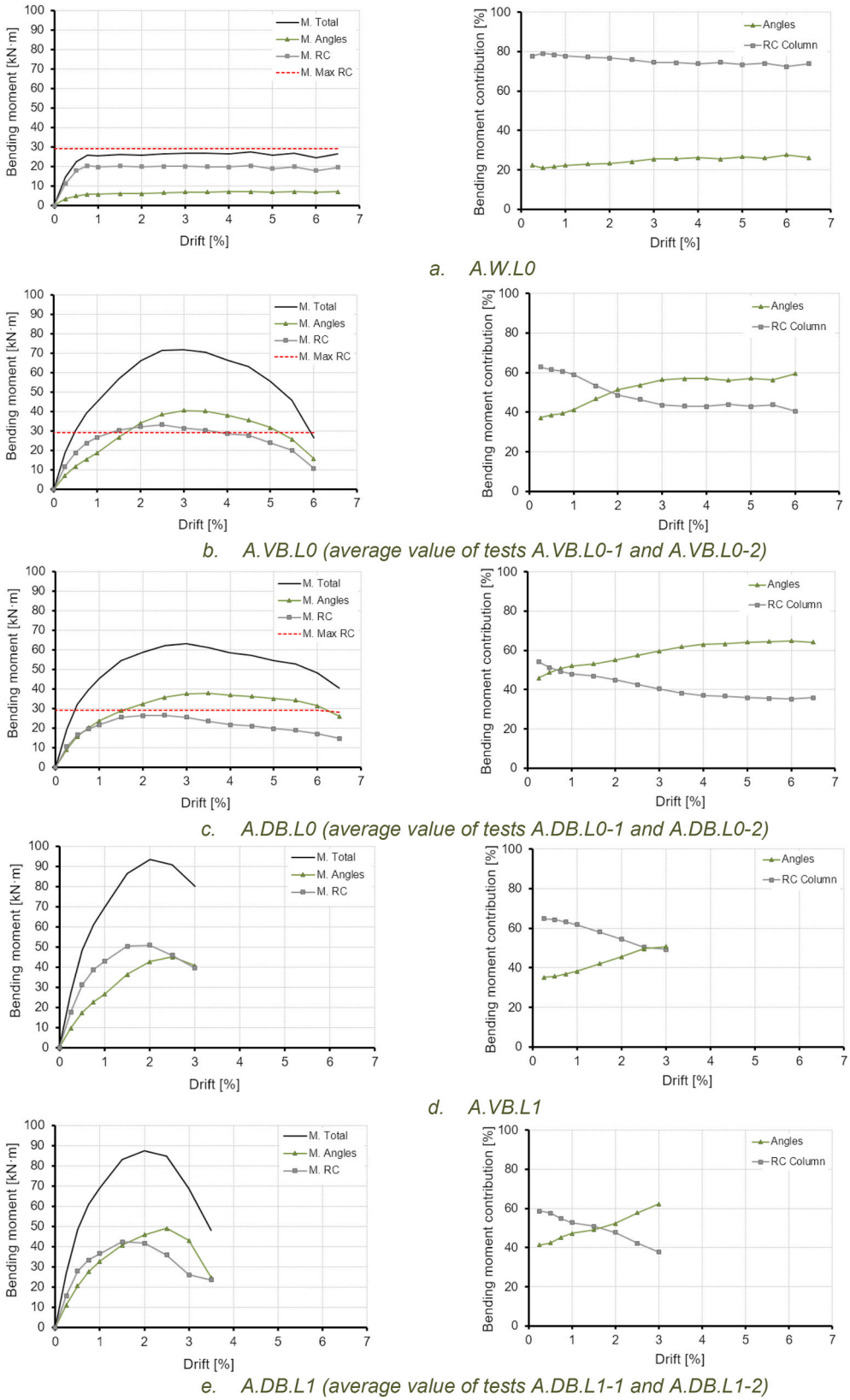

Fig. 13. Behaviour of the composite column section subjected to bending moment (A.W.L0, A.VB.L0 and A.DB.L0) and axial-bending loads (A.VB.L1 and A.DB.L1). On the left, the bending moment resisted by the reinforced concrete section and angles. On the right, the percentage contribution of both elements to the bending moment.

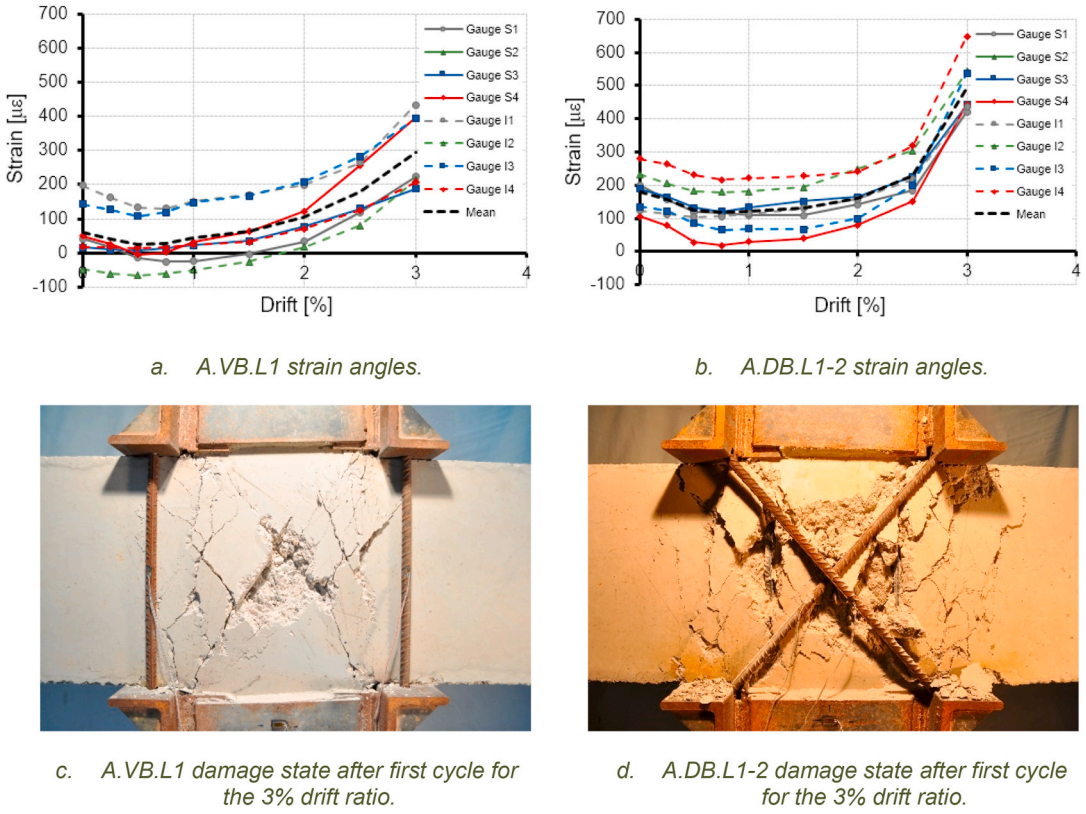

Fig. 14. Longitudinal strain of the eight steel angles (see Fig. 2) of specimens A.VB.L1 and A.DB.L1-2 under gravity load at the end of the first cycle for every drift ratio (a, b) and the damage state of the joints after first cycle for 3% drift ratio (c, d).

the end of the first cycle of the drift ratio indicated on the X-axis (abscissa); it is highlighted here that no horizontal load acted on the specimens at these positions. Despite the gravity load not changing, the strain of the angles increased considerably after some cycles. This was because when the concrete degradation at joint started to become significant (Fig. 14c and d), its axial strength sharply dropped and angles received the load that the joint could not, which prevented collapse. Almost the entire axial load is supported by the steel cage after the 3% drift ratio.

3.5. External bar behaviour

As described above, external bars allowed the capitals to contribute to column strength. External bars connected the steel cage through the joint, which enabled the continuity of column loads. Although the maximum strength of the specimens with vertical or diagonal bars was not that different, the behaviour of both external bars and the joint panel was.

When the beam-column joint was subjected to cyclic loads and the column was strengthened by the steel cage, the weak section of the column was where the column met the joint and the column reinforcement strain peaked (Fig. 11c). Vertical bars always worked no matter what the direction of loads, but diagonal bars worked only when movement occurred in a certain direction (Fig. 15a and Fig. 15b). This does not mean that vertical bars were more effective; diagonal bars were more effective insofar as tension was transferred directly from the column sides where steel angles were in tension. The verticals bars system needed the indirect transmission of loads through the joint to gain equilibrium and, finally, the joint failed (Fig. 8b).

The washers of nuts remained in contact with capitals regardless of movement being to one side or the other when vertical bars were used as bars were in tension. However, when employing diagonal bars, they did not work in one of the two movement directions. So a gap appeared between the washer and the capital (Fig. 15c). The threaded part of bars at their ends was the system's weak part. As ends of bars had a smaller area than the remaining length, this was the part where the most marked deformation of bars concentrated, which reduced the cross-sectional area (necking) of external bars (Fig. 15d). Given the inclination of diagonal bars, these bars were subjected to more tension than vertical bars under the same horizontal load.

4. Conclusions

The analysis of this experimental campaign highlights the influence of joint strengthening on the cyclic response of reinforced concrete beam-column joints. Steel caging can avoid the compression, shear or bending failures of columns. Instead when no connections are made between columns, beam-column joints strength to horizontal loads is limited by column reinforcement yielding at the column-joint interface where the steel cage ends. In relation to this issue, two connection types were employed in the experimental campaign: vertical and diagonal external bars.

When no axial load is applied to columns, the use of capitals with vertical or diagonal bars increases more than doubles the control specimen's strength: 2.5- and 2.2-fold, respectively. In both cases, the contribution of steel angles to the bending moment of the column on the section where angles are monitored (230 mm from the column-joint interface) is around 40–60% of the total bending moment. Although both solutions offer very satisfactory results, it is important to highlight that the failure mode completely changes. During these experimental campaigns, vertical bars increase the column-joint interface bending moment and failure shifts to the joint. If diagonal bars are employed, the bending capacity of the column joint also increases and joint failure is avoided; failure is transferred to the beams. According to these results, diagonal bars strengthening is more appropriate in joints of columns with no axial load (top floors of buildings) in the cases where it is

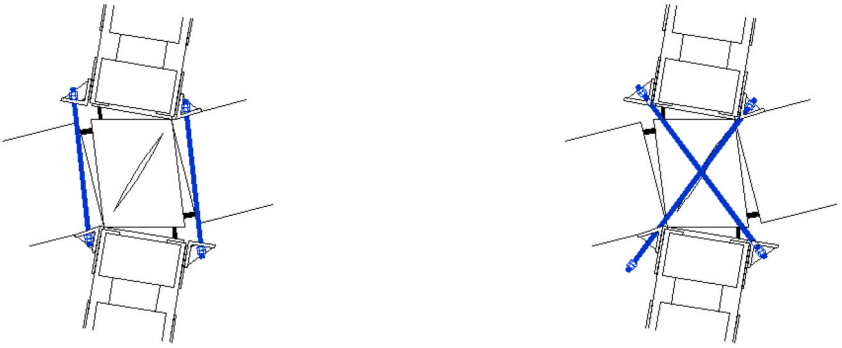

a. Deformation scheme of specimens.

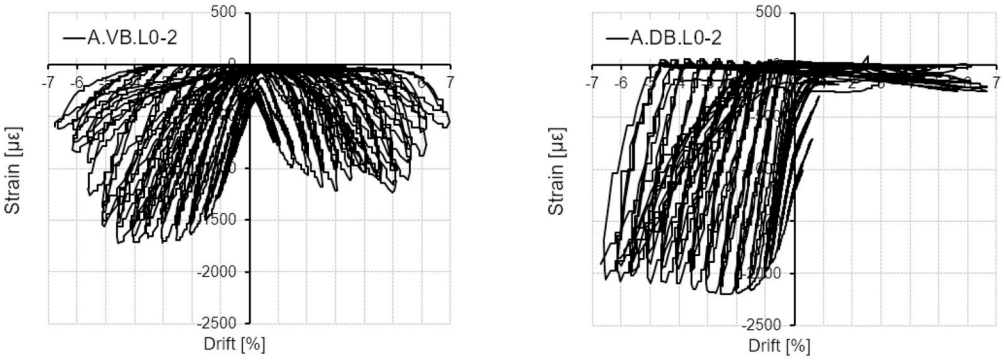

b. Hysteretic loops of the strain on the vertical and diagonal external bars.

c. Contact and loss of contact of capitals in tension-compression reverse cycles.

d. Plastic deformation with the reduction in the cross-sectional area on one diagonal bar

Fig. 15. Behaviour of vertical (A.VB.L0) and diagonal bars (A.DB.L0).

necessary to increase the bending capacity of the columns and the joints are vulnerable to being damaged.

When axial load is applied, no major differences appear between diagonal or vertical external bars. Yet in this case, capitals are more important because they allow increases in both the joint size and mechanical arm of the column. Besides, capitals can avoid the structure from collapsing when the joint is severely damaged.

The strengthening solution herein presented increases beam-column joint strength when the column-joint interface is the weaker part. This case is very common when column strengthening is performed and no

connections of columns through the floor are made. The proposed technique does not involve damaging either beams or the joint of existing reinforced concrete structures: columns are connected with bars placed externally to those elements. This simplifies the application of the technique in practical refurbishment cases when strengthening beam-column joint is needed. This paper also highlights the importance of considering the joint when designing interventions because it can be the weakest element in the strong column-weak beam design. In such situations, vertical bars cannot preserve the joint's integrity, but diagonal bars can, as the present research shows.

Author statement

All authors have participated in the different stages involved in the research performed and manuscript preparation.

Declaration of competing interest

The authors declare that they have no known competing financial interests or personal relationships that could have appeared to influence the work reported in this paper.

Acknowledgements

The authors wish to thank the financial support provided by the Spanish Ministry of Science and Innovation and the Spanish Ministry of Economy and Competitiveness with Research Projects BIA 2008–06268 and RTI2018-099091-B-C22.

References

[1] J. Adam, Global research continues into strengthening structures against earthquakes, Proc. Inst. Civ. Eng. - Civ. Eng. 168 (2015), https://doi.org/10.1680/cien.2015.168.4.148, 148–148.
[2] S. Doocy, A. Daniels, C. Packer, A. Dick, T.D. Kirsch, The human impact of earthquakes: a historical review of events 1980-2009 and systematic literature review, PLoS Curr (2013), https://doi.org/10.1371/currents.dis.67bd14fe457f1db0b5433a8ee20fb833.
[3] S. Demir, M. Günaydin, B. Atmaca, A.C. Altunişik, M. Hüsem, S. Adanur, Z. Angin, S. Ateş, Performance evaluation of reinforced concrete buildings during the sivrice-elazlğ earthquake (M w = 6. 8, january 24, 2020) in accordance with Turkish earthquake code, J. Earthq. Tsunami. (2021), https://doi.org/10.1142/S1793431121500184.
[4] J.G. Ruiz-Pinilla, J.M. Adam, R. Pérez-Cárcel, J. Yuste, J.J. Moragues, Learning from RC building structures damaged by the earthquake in Lorca, Spain, in: 2011, Eng. Fail. Anal. 68, 2016, pp. 76–86, https://doi.org/10.1016/j.engfailanal.2016.05.013.
[5] S. Ates, V. Kahya, M. Yurdakul, S. Adanur, Damages on reinforced concrete buildings due to consecutive earthquakes in Van, Soil Dynam. Earthq. Eng. 53 (2013) 109–118, https://doi.org/10.1016/j.soildyn.2013.06.006.
[6] O. Murat, Field reconnaissance of the october 23, 2011, van, Turkey, earthquake: lessons from structural damages, J. Perform. Constr. Facil. 29 (2015), 04014125, https://doi.org/10.1061/(ASCE)CF.1943-5509.0000532.
[7] P. Ricci, F. de Luca, G.M. Verderame, 6th April 2009 L'Aquila earthquake, Italy: reinforced concrete building performance, Bull. Earthq. Eng. 9 (2011) 285–305, https://doi.org/10.1007/s10518-010-9204-8.
[8] K.H. Jk Bothara, General observations of building behavior during the 8th October 2005 Pakistan earthquake, Bull. N. Z. Soc. Earthq. Eng. 41 (2008) 209–233.
[9] L.D. Decanini, A. De Sortis, A. Goretti, L. Liberatore, F. Mollaioli, P. Bazzurro, Performance of reinforced concrete buildings during the 2002 Molise, Italy, earthquake, Earthq. Spectra 20 (2004) 221–255, https://doi.org/10.1193/1.1765107.
[10] M. Rizwan, N. Ahmad, J. Akbar, B. Ilyas, Arifullah, A. Ali, M.E. Ahmad, S. Pervez, M.E. Rahim, M.A.Z. Khan, Global seismic fragility functions for low-rise RC frames with construction deficiencies, Adv. Civ. Eng. 2020 (2020), https://doi.org/10.1155/2020/3174738.
[11] J. Akbar, N. Ahmad, B. Alam, Seismic strengthening of deficient reinforced concrete frames using reinforced concrete haunch, ACI Struct. J. 116 (2019) 225–236, https://doi.org/10.14359/51710875.
[12] M. Rizwan, S.A.A. Shah, Seismic damage assessment of deficient reinforced concrete frame structures, Civ. Environ. Eng. (2021), https://doi.org/10.2478/cee-2021-0004, 0.
[13] R. Couto, M.V. Requena-García-Cruz, R. Bento, A. Morales-Esteban, Seismic capacity and vulnerability assessment considering ageing effects: case study—three local Portuguese RC buildings, Bull. Earthq. Eng. (2020) 1–24, https://doi.org/10.1007/s10518-020-00955-4.
[14] D. Bru, A. González, F.J. Baeza, S. Ivorra, Seismic behavior of 1960's RC buildings exposed to marine environment, Eng. Fail. Anal. 90 (2018) 324–340, https://doi.org/10.1016/J.ENGFAILANAL.2018.02.011.
[15] A. Bossio, G.P. Lignola, A. Prota, An overview of assessment and retrofit of corroded reinforced concrete structures, in: Procedia Struct. Integr., Elsevier B.V., 2018, pp. 394–401, https://doi.org/10.1016/j.prostr.2018.11.051.
[16] J. Cheng, X. Luo, P. Xiang, Experimental study on seismic behavior of RC beams with corroded stirrups at joints under cyclic loading, J. Build. Eng. 32 (2020) 101489, https://doi.org/10.1016/j.jobe.2020.101489.
[17] C.X. Xu, S. Peng, J. Deng, C. Wan, Study on seismic behavior of encased steel jacket-strengthened earthquake-damaged composite steel-concrete columns, J. Build. Eng. 17 (2018) 154–166, https://doi.org/10.1016/j.jobe.2018.02.010.
[18] J. Garzón-Roca, J. Ruiz-Pinilla, J.M. Adam, P.A. Calderón, An experimental study on steel-caged RC columns subjected to axial force and bending moment, Eng. Struct. 33 (2011) 580–590, https://doi.org/10.1016/j.engstruct.2010.11.016.
[19] M.F. Belal, H.M. Mohamed, S.A. Morad, Behavior of reinforced concrete columns strengthened by steel jacket, HBRC J 11 (2015) 201–212, https://doi.org/10.1016/j.hbrcj.2014.05.002.
[20] P.A. Calderón, J.M. Adam, S. Ivorra, F.J. Pallarés, E. Giménez, Design strength of axially loaded RC columns strengthened by steel caging, Mater. Des. 30 (2009) 4069–4080, https://doi.org/10.1016/j.matdes.2009.05.014.
[21] M. Del Zoppo, M. Di Ludovico, A. Balsamo, A. Prota, G. Manfredi, FRP for seismic strengthening of shear controlled RC columns: experience from earthquakes and experimental analysis, Compos. B Eng. 129 (2017) 47–57, https://doi.org/10.1016/j.compositesb.2017.07.028.
[22] A. Napoli, R. Realfonzo, RC columns strengthened with novel CFRP systems: an experimental study, Polymers 7 (2015) 2044–2060, https://doi.org/10.3390/polym7101499.
[23] S.M. Mourad, M.J. Shannag, Repair and strengthening of reinforced concrete square columns using ferrocement jackets, Cement Concr. Compos. 34 (2012) 288–294, https://doi.org/10.1016/J.CEMCONCOMP.2011.09.010.
[24] T. Chrysanidis, I. Tegos, Axial and transverse strengthening of R/C circular columns: conventional and new type of steel and hybrid jackets using high-strength mortar, J. Build. Eng. 30 (2020) 101236, https://doi.org/10.1016/J.JOBE.2020.101236.
[25] E. Choi, S.H. Park, B.S. Cho, D. Hui, Lateral reinforcement of welded SMA rings for reinforced concrete columns, J. Alloys Compd. 577 (2013), https://doi.org/10.1016/j.jallcom.2012.02.135.
[26] D. Jung, J. Wilcoski, B. Andrawes, Bidirectional shake table testing of RC columns retrofitted and repaired with shape memory alloy spirals, Eng. Struct. 160 (2018) 171–185, https://doi.org/10.1016/j.engstruct.2017.12.046.
[27] A. Ghobarah, A. Biddah, Dynamic analysis of reinforced concrete frames including joint shear deformation, Eng. Struct. 21 (1999) 971–987, https://doi.org/10.1016/S0141-0296(98)00052-2.
[28] D.M. Cotsovos, Cracking of RC beam/column joints: implications for the analysis of frame-type structures, Eng. Struct. 52 (2013) 131–139, https://doi.org/10.1016/J.ENGSTRUCT.2013.02.018.
[29] H. Naderpour, M. Mirrashid, Classification of failure modes in ductile and non-ductile concrete joints, Eng. Fail. Anal. 103 (2019) 361–375, https://doi.org/10.1016/J.ENGFAILANAL.2019.04.047.
[30] A. Borghini, F. Gusella, A. Vignoli, Seismic vulnerability of existing R.C. buildings: a simplified numerical model to analyse the influence of the beam-column joints collapse, Eng. Struct. 121 (2016) 19–29, https://doi.org/10.1016/J.ENGSTRUCT.2016.04.045.
[31] S.G. Walker, Seismic Performance of Existing Reinforced Concrete Beam-Column Joints, University of Washington, 2001.
[32] J. Kim, J.M. LaFave, A simplified approach to joint shear behavior prediction of RC beam-column connections, Earthq. Spectra 28 (2012) 1071–1096, https://doi.org/10.1193/1.4000064.
[33] L.K.A.Z. M Engindeniz, Repair and strengthening of reinforced concrete beam-column joints: state of the art, ACI Struct. J. 102 (2005) 187–197.
[34] C. Xu, S. Peng, X. Liu, C. Wang, Q. Xu, Analysis of the seismic behavior of CFRP-strengthened seismic-damaged composite steel-concrete frame joints, J. Build. Eng. 28 (2020) 101057, https://doi.org/10.1016/j.jobe.2019.101057.
[35] R. Realfonzo, A. Napoli, J.G.R. Pinilla, Cyclic behavior of RC beam-column joints strengthened with FRP systems, Construct. Build. Mater. 54 (2014) 282–297, https://doi.org/10.1016/j.conbuildmat.2013.12.043.
[36] A. De Vita, A. Napoli, R. Realfonzo, Full scale reinforced concrete beam-column joints strengthened with steel reinforced polymer systems, Front. Mater. 4 (2017) 18, https://doi.org/10.3389/fmats.2017.00018.
[37] A. Prota, A. Nanni, G. Manfredi, E. Cosenza, Selective upgrade of underdesigned reinforced beam-column joints using carbon fiber-reinforced concrete, ACI Struct. J. 101 (2004) 699–707.
[38] S. Sasmal, K. Ramanjaneyulu, B. Novák, V. Srinivas, K. Saravana Kumar, C. Korkowski, C. Roehm, N. Lakshmanan, N.R. Iyer, Seismic retrofitting of nonductile beam-column sub-assemblage using FRP wrapping and steel plate jacketing, Construct. Build. Mater. 25 (2011) 175–182, https://doi.org/10.1016/J.CONBUILDMAT.2010.06.041.
[39] E. Ilia, D. Mostofinejad, Seismic retrofit of reinforced concrete strong beam–weak column joints using EBROG method combined with CFRP anchorage system, Eng. Struct. 194 (2019) 300–319, https://doi.org/10.1016/j.engstruct.2019.05.070.
[40] K. Sakthimurugan, K. Baskar, Experimental investigation on rcc external beam-column joints retrofitted with basalt textile fabric under static loading, Compos. Struct. 268 (2021) 114001, https://doi.org/10.1016/j.compstruct.2021.114001.

[41] S. Villar-Salinas, A. Guzmán, J. Carrillo, Performance evaluation of structures with reinforced concrete columns retrofitted with steel jacketing, J. Build. Eng. 33 (2021) 101510, https://doi.org/10.1016/j.jobe.2020.101510.
[42] M. Kazem Sharbatdar, A. Kheyroddin, E. Emami, Cyclic performance of retrofitted reinforced concrete beam–column joints using steel prop, Construct. Build. Mater. 36 (2012) 287–294, https://doi.org/10.1016/J.CONBUILDMAT.2012.04.115.
[43] J. Shafaei, A. Hosseini, M.S. Marefat, Seismic retrofit of external RC beam–column joints by joint enlargement using prestressed steel angles, Eng. Struct. 81 (2014) 265–288, https://doi.org/10.1016/J.ENGSTRUCT.2014.10.006.
[44] G. Campione, L. Cavaleri, M. Papia, Flexural response of external R.C. beam–column joints externally strengthened with steel cages, Eng. Struct. 104 (2015) 51–64, https://doi.org/10.1016/J.ENGSTRUCT.2015.09.009.
[45] A. Kheyroddin, E. Emami, A. Khalili, RC beam–column connections retrofitted by steel prop: experimental and analytical studies, Int. J. Civ. Eng. 18 (2020) 501–518, https://doi.org/10.1007/s40999-019-00481-8.
[46] A. Maddah, A. Golafshar, M.H. Saghafi, 3D RC beam–column joints retrofitted by joint enlargement using steel angles and post-tensioned bolts, Eng. Struct. 220 (2020) 110975, https://doi.org/10.1016/j.engstruct.2020.110975.
[47] Ö. Yurdakul, Ö. Avşar, Strengthening of substandard reinforced concrete beam-column joints by external post-tension rods, Eng. Struct. 107 (2016) 9–22, https://doi.org/10.1016/j.engstruct.2015.11.004.
[48] A. Torabi, M.R. Maheri, Seismic repair and retrofit of RC beam-column joints using stiffened steel plates, Iran, J. Sci. Technol. - Trans. Civ. Eng. 41 (2017) 13–26, https://doi.org/10.1007/s40996-016-0027-y.
[49] M. Khodaei, M.H. Saghafi, A. Golafshar, Seismic retrofit of exterior beam-column joints using steel angles connected by PT bars, Eng. Struct. 236 (2021) 112111, https://doi.org/10.1016/j.engstruct.2021.112111.
[50] X. Liu, T. Gernay, L. zhi Li, Z. dao Lu, Seismic performance of post-fire reinforced concrete beam-column joints strengthened with steel haunch system, Eng. Struct. 234 (2021) 111978, https://doi.org/10.1016/j.engstruct.2021.111978.
[51] J. Akbar, N. Ahmad, M. Rizwan, S. Javed, B. Alam, Response modification factor of RC frames strengthened with RC haunches, Shock Vib. 2020 (2020), https://doi.org/10.1155/2020/3835015.
[52] A. Pimanmas, P. Chaimahawan, Cyclic shear resistance of expanded beam-column joint, Procedia Eng 14 (2011) 1292–1299, https://doi.org/10.1016/J.PROENG.2011.07.162.
[53] E.S. Lam, B. Li, Z. Xue, K. Leung, J.Y. Lam, Experimental studies on reinforced concrete interior beam-column joints strengthened by unsymmetrical chamfers, Eng. Struct. 191 (2019) 575–582, https://doi.org/10.1016/J.ENGSTRUCT.2019.03.099.
[54] J.G. Ruiz-Pinilla, A. Cladera, F.J. Pallarés, P.A. Calderón, J.M. Adam, RC columns strengthened by steel caging: cyclic loading tests on beam-column joints with non-ductile details, Construct. Build. Mater. 301 (2021) 124105, https://doi.org/10.1016/J.CONBUILDMAT.2021.124105.
[55] Eh-80, Instrucción para el proyecto y ejecución de obras de hormigón en masa o armado, 1980.
[56] E. Giménez, J.M. Adam, S. Ivorra, P.A. Calderón, Influence of strips configuration on the behaviour of axially loaded RC columns strengthened by steel angles and strips, Mater. Des. 30 (2009) 4103–4111, https://doi.org/10.1016/j.matdes.2009.05.010.
[57] J.M. Adam, S. Ivorra, F.J. Pallarés, E. Giménez, P.A. Calderón, Axially loaded RC columns strengthened by steel caging. Finite element modelling, Construct. Build. Mater. 23 (2009) 2265–2276, https://doi.org/10.1016/J.CONBUILDMAT.2008.11.014.
[58] A. Beres, S.P. Pessiki, R.N. White, P. Gergely, Implications of experiments on the seismic behavior of gravity load designed RC beam-to-column connections, Earthq. Spectra 12 (1996) 185–198, https://doi.org/10.1193/1.1585876.
[59] S. Hakuto, R. Park, H. Tanaka, Seismic load tests on interior and exterior beam-column joints with substandard reinforcing details, ACI Struct. J. 97 (2000) 11–25.
[60] H. Yang, W. Zhao, Z. Zhu, J. Fu, Seismic behavior comparison of reinforced concrete interior beam-column joints based on different loading methods, Eng. Struct. 166 (2018) 31–45, https://doi.org/10.1016/j.engstruct.2018.03.022.